

Comparative analysis of genomic characteristics, fitness and virulence of MRSA ST398 and ST9 isolated from China and Germany

Xing Ji^{a*}, Henrike Krüger^{b*}, Jin Tao^a, Yaxin Wang^a, Andrea T. Feßler^b, Rina Bai^a, Shaolin Wang^a, Yanjun Dong^a, Jianzhong Shen^a, Yang Wang^a, Stefan Schwarz^{a,b} and Congming Wu^a

^aBeijing Key Laboratory of Detection Technology for Animal-Derived Food Safety, College of Veterinary Medicine, China Agricultural University, Beijing, People's Republic of China; ^bDepartment of Veterinary Medicine, Institute of Microbiology and Epizootics, Centre for Infection Medicine, Freie Universität Berlin, Berlin, Germany

ABSTRACT

Methicillin-resistant *Staphylococcus aureus* (MRSA) of sequence types ST398 and ST9 are dominant lineages among livestock in Europe and Asia, respectively. Although both STs were commonly found as colonizers of the skin and the mucosal membranes, MRSA ST398, rather than MRSA ST9, has been reported to cause infections in humans and animals. Herein, we comparatively analyzed the genomic characteristics, fitness and virulence of MRSA ST398 and ST9 isolated from pigs in both China (CHN) and Germany (GER) to explore the factors that lead to differences in their epidemics and pathogenicity. We observed that the CHN-MRSA ST9 and the GER-MRSA ST9 have evolved independently, whereas the CHN-MRSA ST398 and GER-MRSA ST398 had close evolutionary relationships. Resistance to antimicrobial agents commonly used in livestock, the enhanced ability of biofilm formation, and the resistance to desiccation contribute to the success of the dominant clones of CHN-MRSA ST9 and GER-MRSA ST398, and the *vwb*^{vSaα} gene on the genomic island might in part contribute to their colonization fitness in pigs. All MRSA ST398 strains revealed more diverse genome structures, higher tolerance to acids and high osmotic pressure, and greater competitive fitness in co-culture experiments. Notably, we identified and characterized a novel *hysA*^{vSaβ} gene, which was located on the genomic island vSaβ of MRSA ST398 but was absent in MRSA ST9. The enhanced pathogenicity of the MRSA ST398 strains due to *hysA*^{vSaβ} might in part explain why MRSA ST398 strains are more likely to cause infections.

ARTICLE HISTORY Received 20 May 2021; Revised 29 June 2021; Accepted 29 June 2021

KEYWORDS MRSA; genome; fitness; virulence; pig; ST398; ST9

Introduction

Since the mid-2000s, livestock-associated methicillin-resistant *Staphylococcus aureus* (LA-MRSA) has been identified among pigs worldwide. The reports of LA-MRSA have increased enormously due to its increasing antimicrobial resistance and potential threats for zoonotic infections [1]. Molecular analysis of the LA-MRSA strains by multi-locus sequence typing identified ST398 as the dominant lineage in European countries, Australia as well as North and South America, whereas ST9 was dominant in Asian countries, especially in China [2,3]. In contrast, non-successfully colonizing strains of LA-MRSA ST9 in European countries and LA-MRSA ST398 in China were sporadically isolated [4,5].

MRSA ST398 originated from human-associated methicillin-susceptible *S. aureus* (MSSA) ST398, which acquired the *mecA*-carrying elements SCCmecV or SCCmecIV and lost the φSa3 phage carrying the human immune evasion cluster (IEC)

including the genes *sak*, *scn*, and *chp* to adapt to and spread successfully among pigs [6]. MRSA ST398 also acquired the tetracycline resistance genes *tet(K)* and *tet(M)*, and the cadmium/zinc resistance gene *czrC* to better adapt to the selection pressure imposed by tetracyclines and zinc, both commonly used in the pig breeding industry [7]. MRSA ST398 was not particularly host-specific as it was found not only in pigs, but also in cattle, horses, rabbits, poultry and humans among others [3], most likely transferred via direct contact, the food chain or environmental routes. MRSA ST398 can cause a wide range of infections, such as abscesses, pneumonia, skin and soft tissue infections (SSTI), and bacteremia, in humans with or without animal contact, and the trend of this transmission seems to be increasing [8–10]. In contrast, most LA-MRSA ST9 in China were isolated from pigs and cattle, which carried the novel SCCmecXII element and a multiple antibiotic resistance gene cluster comprising the genes *aadE-spw-lsa(E)-lnu(B)* [11–13]. Human

CONTACT Yang Wang  wangyang@cau.edu.cn; Stefan Schwarz  stefan.schwarz@fu-berlin.de; Congming Wu  wucm@cau.edu.cn

 Supplemental data for this article can be accessed <https://doi.org/10.1080/22221751.2021.1951125>

*These authors contributed equally to this study.

© 2021 The Author(s). Published by Informa UK Limited, trading as Taylor & Francis Group.

This is an Open Access article distributed under the terms of the Creative Commons Attribution-NonCommercial License (<http://creativecommons.org/licenses/by-nc/4.0/>), which permits unrestricted non-commercial use, distribution, and reproduction in any medium, provided the original work is properly cited.

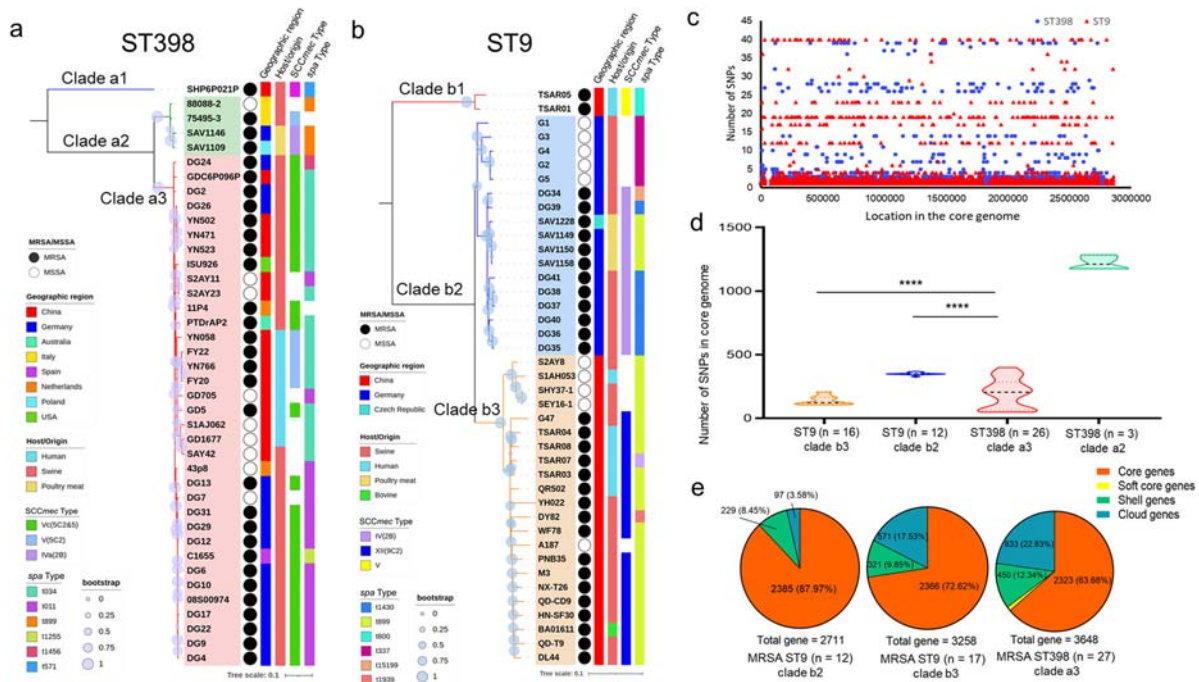


Figure 1. Analysis of molecular evolution characteristics. (a) Core-genome SNPs phylogenetic trees of ST398. (b) Core-genome SNPs phylogenetic trees of ST9. (c) Distribution of SNPs in the phylogenetic trees of ST9 and ST398. (d) Number of SNPs per strain in each main clade of ST9 and ST398. Only MRSA strains were used in each clade. (e) Number of accessory and core genes of MRSA ST9 and MRSA ST398 in each main clade.

infections caused by MRSA ST9 have rarely been reported [14].

Previous studies have contributed to our understanding of the epidemiological, genetic and pathogenic characteristics of successful MRSA ST398 or ST9 strains. However, the characteristics of epidemiologically non-successful MRSA ST9 and ST398 strains, the specific factors that contribute to the prevalence of dominant MRSA ST9 or ST398 in different regions, and the reasons of the frequent infections of humans and animals caused by MRSA ST398 remain to be elucidated. Herein, we compared and analyzed the genomic characteristics, fitness and virulence properties of ST9 and ST398 strains isolated from pigs in China and Germany to better understand the epidemiologically successful porcine MRSA lineages.

Results

Phylogenetic analysis based on core genome SNPs of *S. aureus* ST9 and ST398

All ST398 strains (China $n = 16$, Germany $n = 16$, other countries $n = 8$) were divided into three phylogenetic clades (Figure 1(a)). The CHN- ($n = 9$) and nearly all of GER- ($n = 14$) MRSA ST398 strains clustered in the same clade a3 which also includes ST398 strains ($n = 5$) from the USA, Australia, and other European countries. All MRSA ST398 of clade a3 carried *SCCmecV* or its subtype, and the main *spa* types were t034 and t011. The ST9 strains (China $n = 24$, Germany $n = 16$, other countries $n = 1$) were also

divided into three phylogenetic clades (Figure 1(b)), most CHN-MRSA ST9 ($n = 17$) clustered in clade b3, while all GER-MRSA ST9 ($n = 11$) clustered in clade b2. Within clade b3, most MRSA ST9 were *spa* type t899 and carried the novel *SCCmecXII* element, while most MRSA ST9 ($n = 10$) of clade b2 harboured *SCCmecIV* with *spa* types t1430 or t899. These results suggest that porcine CHN-MRSA ST398 and GER-MRSA ST398 belong to the same ancestral lineage, whilst porcine MRSA ST9 strains from China and Germany belong to two independent evolutionary lineages.

Genomic characteristics of MRSA ST398 and ST9

Based on the core-genome phylogenetic tree, we identified and found that core genome SNPs of MRSA ST398 and ST9 in the major clades uniformly covered the whole genome, without high-frequency mutation regions (Figure 1(c)). The number of SNPs in the MRSA ST9 clades b2 and b3 ranged between 346–366 (coefficient of variation, CV = 2.029%) and 95–203 (CV = 23.920%), respectively, whilst the number of SNPs in the MRSA ST398 clades a2 and a3 ranged between 1179–1287 (CV = 4.401%) and 49–362 (CV = 60.940%). Particularly, we identified 137 SNPs (94 nonsynonymous [dN] and 43 synonymous [dS] SNPs; dN/dS ratio 2.2) in the core genome of CHN and GER-MRSA ST398 representative strains (08S00974 and GDC6P096P), and the genes with

high dN SNPs were mainly enriched in the categories of cell signalling, information storage, and processing, including the categories L (replication, recombination, and repair), M (cell wall/membrane/envelope biogenesis) and D (cell cycle control, cell division, chromosome partitioning). Correspondingly, we observed 233 SNPs (162 dN and 71 dS SNPs; dN/dS ratio 2.3) in the core genome of CHN and GER-MRSA ST9 strains (QD-CD9 and DG36), high nonsynonymous mutations were mainly enriched in metabolism functions, including categories G (carbohydrate transport and metabolism), H (coenzyme transport and metabolism), and E (amino acid transport and metabolism) (Figure S2). At the whole genome level, we found that the 1283 accessory genes accounting for 35.17% of the total genome of MRSA ST398 in clade a3 were significantly higher than the 326 and 892 accessory genes (12.03% and 27.38%) in MRSA ST9 in clades b2 and b3 ($p < 0.0001$, Figure 1(e)), these accessory genes are mainly composed of mobile genetic elements (MGEs), including SCC_{mec} elements, antimicrobial resistance genes, and prophages, which are also the main differences in the genome of the representative strains of MRSA ST398 and ST9 from China and Germany (Table S1, Figures S3(a, b) and S4(a,b)).

Antimicrobial resistance (AMR) pheno- and genotypes of MRSA ST9 and ST398

The antimicrobial resistance profiles of MRSA ST9 and ST398 strains from China were more complex than those from Germany (Figure 2(a)). All CHN-MRSA ST9 and ST398 strains exhibited resistance to clindamycin, erythromycin, tetracycline, tiamulin, virginiamycin M1 and trimethoprim. The resistance rates of CHN-MRSA ST9 to gentamicin (100% vs 20%), ciprofloxacin (96.7% vs 20%), and florfenicol (100% vs 40%) were significantly higher than those of CHN-MRSA ST398 ($p < 0.01$, Table S2). Moreover, CHN-MRSA ST398 showed higher resistance to virginiamycin M1 (100% vs 10%) and tiamulin (100% vs 16.7%) than GER-MRSA ST398 ($p < 0.001$, Table S2). The resistance rates of GER-MRSA ST398 to tetracycline (100% vs 12.5%) and minocycline (100% vs 0%) were significantly higher than those of GER-MRSA ST9. All tested strains were susceptible to tigecycline, linezolid, vancomycin, while minocycline resistance was observed exclusively in all MRSA ST398 strains from CHN and GER. Correspondingly, all tested strains carried multiple antimicrobial resistance genes, but the number and distribution of these genes were different (Figure 2(b,c)). The AMR gene numbers were significantly higher in CHN-MRSA ST9 than in the other three groups ($p < 0.001$). Moreover, many AMR genes were associated with specific strains, such as the phenicol resistance gene *fexA*

and the macrolide, lincosamide and streptogramin B (MLS_B) resistance gene *erm(C)* and the multi-resistance gene cluster *aadE-spw-lsa(E)-lnu(B)* which were significantly more frequently seen in CHN-MRSA ST9 whereas the tetracycline resistance genes *tet(K)* and *tet(M)* were significantly associated with CHN- and GER-MRSA ST398 ($p < 0.01$).

Biofilm formation, physicochemical pressure resistance and competitive ability of MRSA ST9 and ST398

To understand whether there are differences among MRSA ST398 and ST9 strains from China and Germany in their ability to form biofilms, their resistance to physicochemical pressures and their ability to outcompete other strains in co-cultivation assays, five strains from each group were selected according to criteria presented in Figure S1 for further studies. The biofilm forming ability of CHN-MRSA ST9 and GER-MRSA ST398 was significantly higher than that of CHN-ST398 and GER-ST9, respectively ($p < 0.05$, Figure 3(a)). Under desiccation conditions, the survival rate at 96 and 144 h of CHN-MRSA ST9 and GER-MRSA ST398 was significantly increased compared to the other two groups ($p < 0.05$, Figure 3(b) and Table S3). Under acidic conditions, all MRSA ST9 displayed a reduced growth rate compared with MRSA ST398 during the exponential phase ($p < 0.05$, Table S4), while all strains did not show significant differences in their growth rates under alkaline conditions (Figure 3(c)). In a hypertonic environment, the survival rates of all four groups of MRSA were decreased, but the survival at high osmolarity was increased among the CHN- and GER-MRSA ST398, especially when compared to CHN-MRSA ST9 ($p < 0.05$, Figure 3(d)). A switch from physiological conditions to direct exposure to 60°C caused the death of almost all bacteria. After pre-exposure at 48°C, the survival rate at 60°C significantly increased. Unexpectedly, GER-MRSA ST9 strains showed significantly enhanced heat resistance under both conditions, compared to other strains ($p < 0.01$, Table S5, Figure S5(a)). Finally, CHN- and GER-MRSA ST9 showed non-significantly enhanced antioxidant activity at the medical concentration (3%) and at a lower concentration (1.5%) of hydrogen peroxide (Figure S5(b) and Table S6).

In independent growth experiments, the GER-MRSA ST9 strains had a shorter lag phase and a higher growth rate than the strains of the other three groups ($p < 0.05$, Figure 4(a) and Table S7). In co-cultivation experiments (Figures 4(b–f)), CHN-MRSA ST9 revealed a lower growth rate, with significantly decreased viable bacteria after 6 h compared with the other three groups ($p < 0.05$, Table S8). GER-MRSA

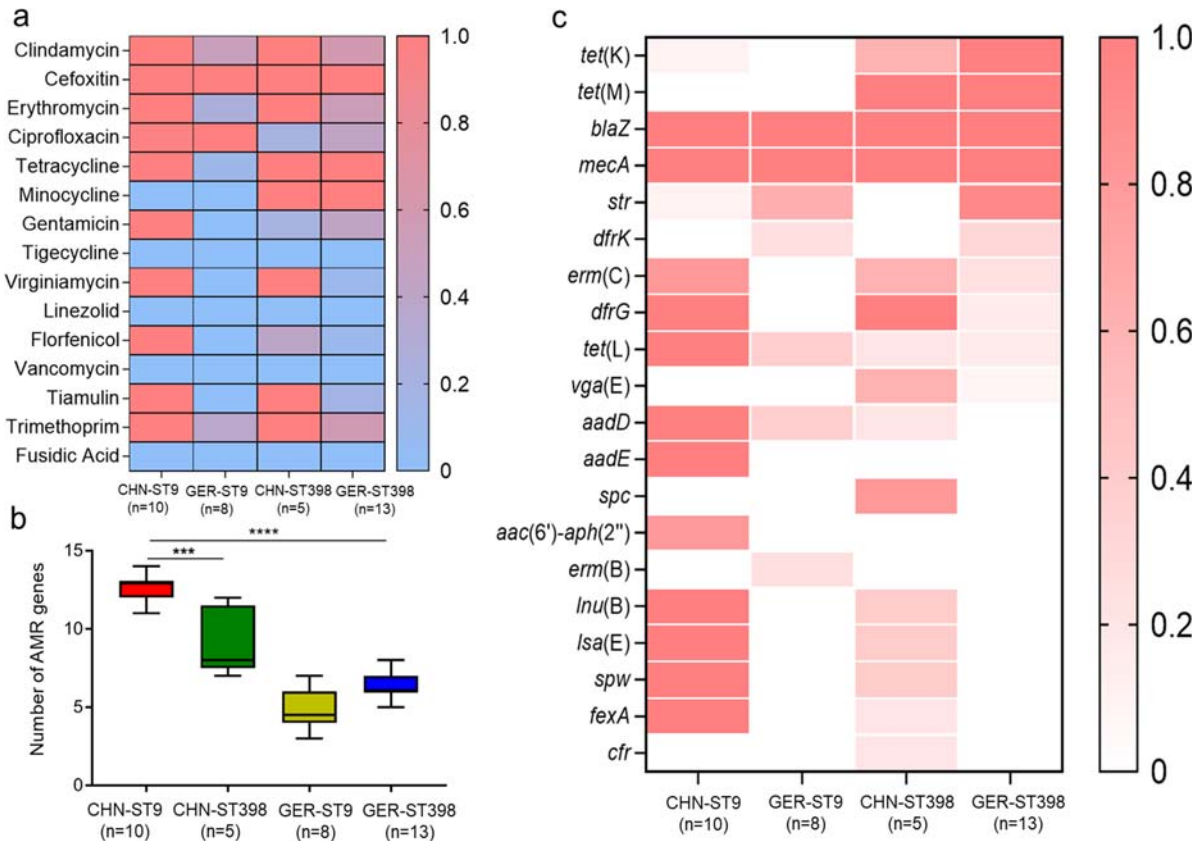


Figure 2. Analysis of antibiotic resistance and resistance genes of MRSA ST9 and MRSA ST398. (a) Heat map of antibiotic resistance properties. (b) Number of antibiotic resistance genes. (c) Heat map of resistance genes. Each cell in the heat map indicates the percentage of strains resistant to specific antibiotics or containing particular resistance genes.

ST398 did not show significant differences in its growth rate and viable bacteria count compared with CHN-MRSA ST398 and GER-MRSA ST9.

MRSA ST398 exhibited higher virulence than MRSA ST9

Furthermore, we selected one representative strain from each of the four different MRSA groups according to the criteria shown in Figure S1 to evaluate the virulence characteristics of MRSA ST9 and ST398 from CHN and GER. In the *Galleria mellonella* larva infection model, both CHN- and GER-MRSA ST9 isolates showed significantly lower lethality than the CHN- and GER-MRSA ST398 strains ($p < 0.05$, Figure 5(a)). Larvae infected with MRSA ST398 had the largest bacterial load, which was significantly different from those infected with MRSA ST9 ($p < 0.05$, Figure 5(b)), suggesting that the enhanced virulence of MRSA ST398 was positively correlated with the high bacterial loads. The mouse skin infection assays showed that the areas and volumes of abscesses caused by MRSA ST398 were significantly larger than those caused by MRSA ST9 ($p < 0.001$), indicating that MRSA ST398 had high virulence and cause more expanded skin damages in mice (Figure 5(c)). However, the common virulence genes carried by MRSA ST398 and ST9 strains were similar, except for the enterotoxin gene

clusters (*seg*, *sei*, *sem*, *sen*, *seo*, *seu*) present only in CHN- and GER-MRSA ST9. Moreover, the gene *cna* coding for the collagen-binding protein was observed only in CHN- and GER-MRSA ST398 (Figure 5(d)). Further comparative WGS analysis showed that, in addition to small-scale variations comprising the presence/absence of one or more genes (Table S9), large-scale variations comprising the presence of prophages and genomic islands were also observed among the MRSA ST9 and ST398 strains included in this study (Figures S3(a,b), S4(a,b)). However, no virulence genes that may increase pathogenicity were identified in the prophages of MRSA ST398. Considering that genomic islands play an important role in the virulence or fitness of *S. aureus*, we further focused on the structural differences of the two genomic islands vSaa and vSa β in detail.

Vwb^{vSaa} located on the novel pathogenicity islands SaPIpig1 and SaPIpig2 revealed unique abilities of pig plasma coagulation

The genomic island vSaa in MRSA ST9 and ST398 was located downstream of the glutamine synthase gene *guaA*. All CHN- and GER-MRSA ST9 ($n = 18$) carried the same genomic island vSaa with an approximate size of ~42 kb. Three different vSaa subtypes were identified in the 38 sequenced CHN- and GER-

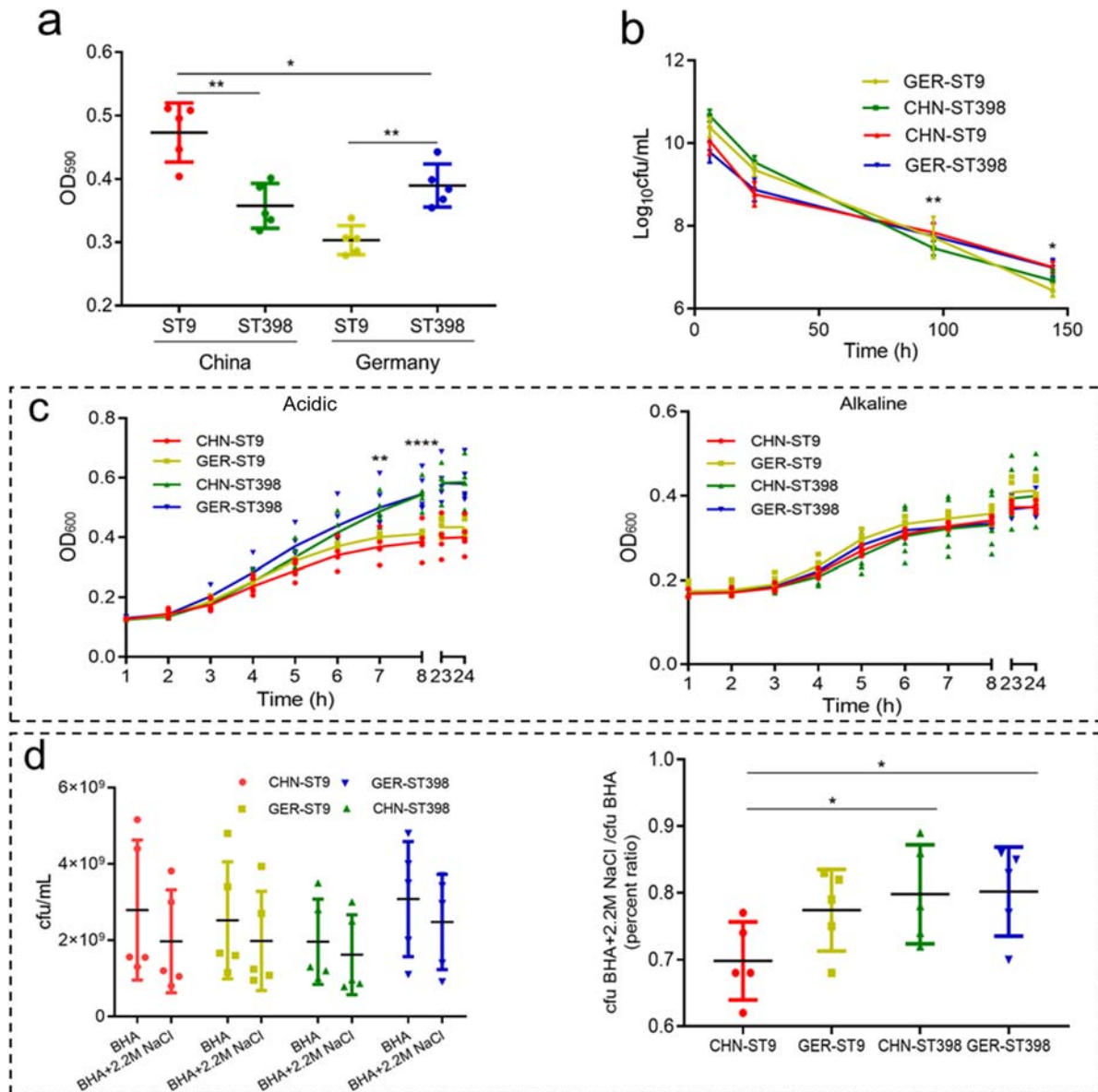


Figure 3. Fitness to physical or chemical pressure analysis. (a) The OD₅₉₀ values of the four groups of strains represent the ability of biofilm formation. (b) Counts (log₁₀ cfu/mL) of the four groups of strains maintained for 144 h after desiccation, with five different strains in each group. (c) Growth characteristics of the four groups of strains under acidic and alkaline conditions. (d) The average cfu of four groups in the presence or absence of 2.2 M NaCl. The average percentage ratio between the cfu counted in the presence and absence of NaCl for each strain tested.

MRSA ST398 strains (Figure 6(a)), and accounted for 39.4% (type 1, $n = 15$), 42.1% (type 2, $n = 16$) and 18.4% (type 3, $n = 7$). A SaPIbov4-like element, flanked by two direct repeat sequences (DRs, 5'-GAGTGGGAATAATTATATATA-3'), was inserted in vSaa of ST9 ($n = 18$), and vSaa subtypes 1 ($n = 15$) and 2 ($n = 16$) of ST398. The SaPIbov4-like elements in ST9 vSaa and ST398 vSaa subtype 1 shared 74.3% nucleotide sequence identity with the previously reported pathogenicity island SaPIbov4 (GenBank number: HM211303.1), therefore, this SaPIbov4-like element was designated SaPIpig1 (GenBank number: MW589252). Moreover, the SaPIbov4-like element in ST398 vSaa subtype 2, which exhibited 57.0% and 60.41% nucleotide sequence identity compared with SaPIpig1 and SaPIbov4, respectively, was designated

SaPIpig2 (GenBank number: MW589253). Both SaPIpig1 and SaPIpig2 elements harboured the von Willibrand factor-binding protein-encoding gene *vwb* (*vwb*^{vSaa}), which had a conserved homologue in the chromosomal DNA (*vwb*^{chr}). The phylogenetic analysis of the Vwb proteins showed that all Vwb^{vSaa} variants clustered together and were distantly related from the Vwb^{chr} proteins, which clustered in another two evolutionary clades (Figure S6(a)). It is noteworthy that the Vwb^{vSaa} carried in the SaPIpig1 and SaPIpig2 are indistinguishable in their amino acid composition to that carried in SaPIbov4. This protein has been confirmed to have a specific coagulation effect on ruminant plasma, but it is not clear whether it also has the same effect on pig plasma [15]. Thus, the clotting ability of representative strains of MRSA

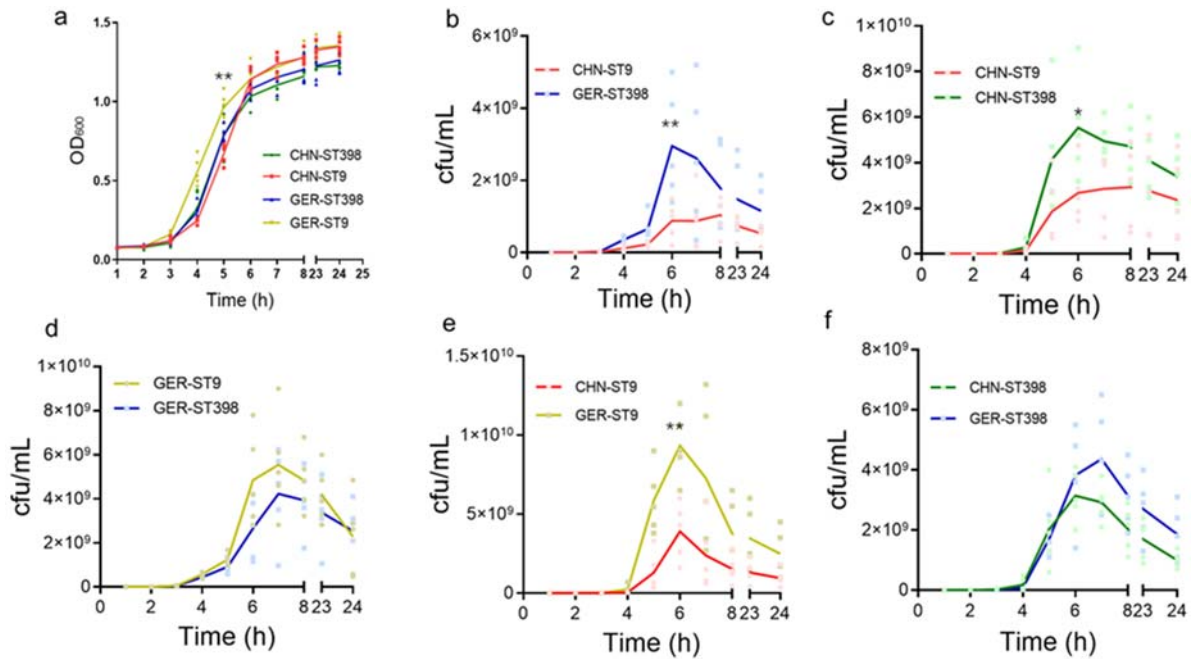


Figure 4. Growth measures from independent cultures and co-culture. (a) Independent growth curve of the strains from the four groups. (b, c, d, e and f) co-culture growth curves of five individual strains randomly paired in each group.

ST398 ($n=6$) and ST9 ($n=4$) to pig, sheep, and bovine plasma was tested (Table S10). We found that strains lacking *vwb*^{vSaα} had no coagulation ability to all three kinds of plasma, whereas the *vwb*^{vSaα} gene-positive strains could coagulate all kinds of animal plasma tested within one hour. This indicated that the *vwb*^{vSaα} confers a unique coagulation ability, not only for ruminant plasma but also for pig and sheep plasma.

HysA^{vSaβ} on genomic island vSaβ enhances the pathogenicity of MRSA ST398

The genomic island vSaβ of MRSA ST9 and MRSA ST398 was located downstream of a conserved tRNA cluster in the chromosomal DNA (Figure 6(b)). All MRSA ST9 strains carried the same ~26 kb genomic island vSaβ, which harboured an enterotoxin gene cluster (*egc*), a repair system encoded by the genes *hsdM* and *hsdS*, but lacked the hyaluronate lyase coding gene *hysA* homologue and serine protease genes. In contrast, the CHN- and GER-MRSA ST398 strains carried a smaller highly conserved vSaβ-related genomic island of ~16.8 kb, which lacked the *egc* cluster, but harboured a *hysA*-like gene, which exhibited 80.4% nucleotide sequence identity and 75.7% amino acid identity to the conserved *hysA* homologous gene/protein in the chromosomal DNA (*hysA*^{chr}/HysA^{chr}) of MRSA ST398. Therefore, we designated this vSaβ-located *hysA* gene as *hysA*^{vSaβ}. The amino acid phylogenetic tree analysis revealed that the HysA^{vSaβ} belonged to an independent evolutionary branch (Figure S6(b)), and was closely related to the corresponding protein from the lineage MRSA

ST504 (M3783C), which often caused mastitis in dairy cattle, and the classical highly virulent hospital-associated MRSA ST36 (MRSA252) [16,17]. The amino acid sequence alignment revealed that the catalytic sites of HysA^{vSaβ} (His299/Tyr308) and HysA^{chr} (His298/Tyr307) are conserved and consistent with that of the hyaluronidase in *Streptococcus agalactiae* [18] (Figure S7). The homologous modelling and molecular docking analysis of HysA^{vSaβ} and HysA^{chr} indicated that the protein simulation structures of HysA^{vSaβ} and HysA^{chr} were similar, and the shape and position of the catalytic pocket are also basically the same. The key amino acid residues within the catalytic centre of HysA^{vSaβ} and HysA^{chr} were identical to that in *S. agalactiae* (1F1S), and their molecular binding capacities were -8.40, -8.31 and -7.53 kcal/mol, respectively. These results suggested that HysA^{vSaβ} and HysA^{chr} may play a catalytic role through the same mechanism with similar binding stability to the hyaluronic acid substrate.

Functional verification was performed to evaluate if the *hysA*^{vSaβ} might play an important role in the pathogenicity of MRSA ST398. Neither *hysA*^{vSaβ} knockout nor *hysA*^{vSaβ} supplementation showed distinct effects on the growth of the respective strains (Figure S8) and we confirmed that both HysA^{chr} and HysA^{vSaβ} had HA decomposing activities. Strains carrying only one *hysA* homologous gene can form a HA decomposition ring (Figure 7(a)). However, the expression of the *hysA*^{vSaβ} gene significantly enhanced the ability of HA decomposition of strain DG29 (Figure 7(b)). In the *Galleria mellonella* larva model, the mortality of larvae infected with and the bacterial load at 48 h of strain DG29 carrying the

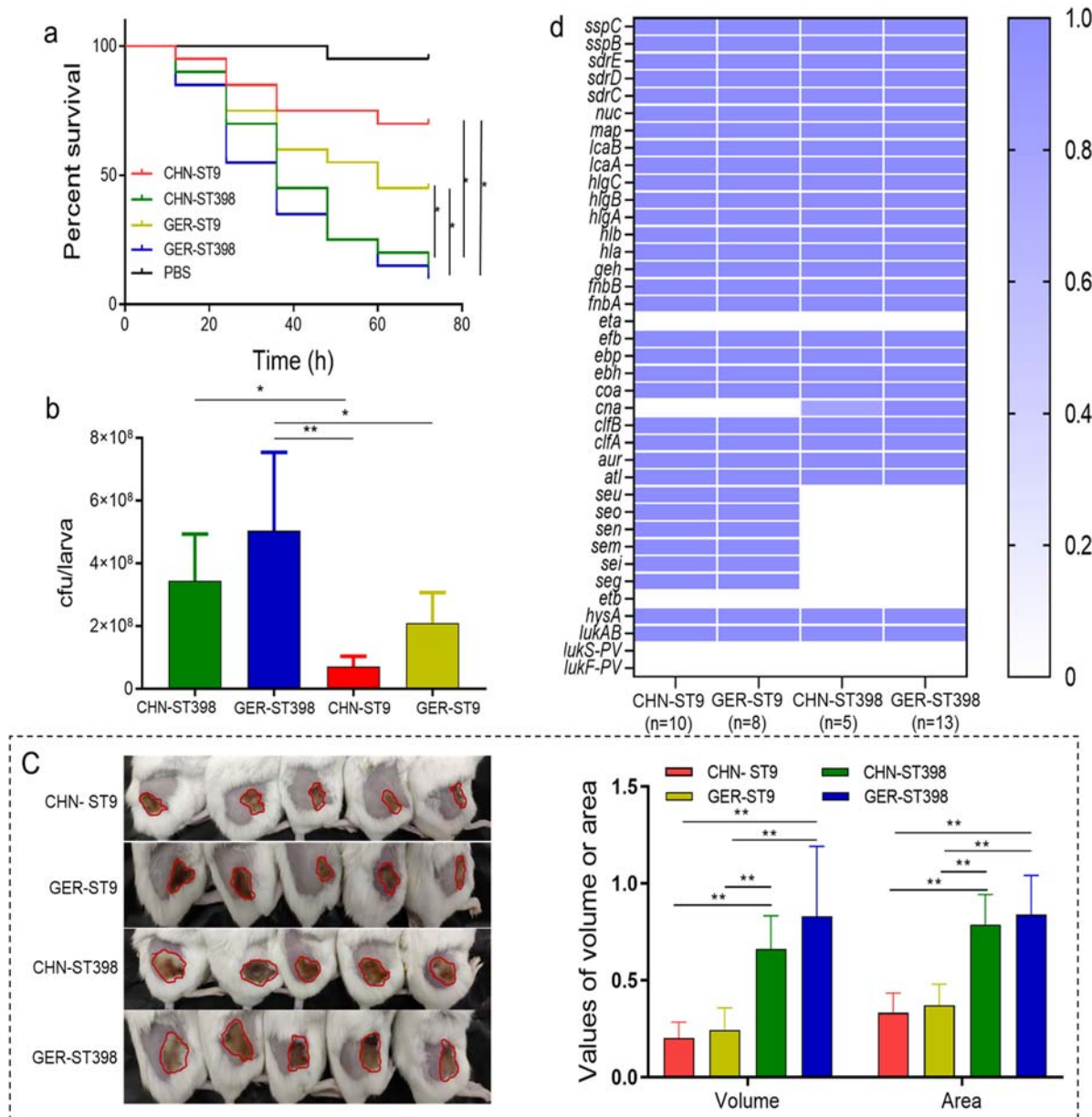


Figure 5. Comparative analysis of virulence and virulence genes. (a) Survival curve of *Galleria mellonella* larvae, 10 larvae infected with each strain were used and the mortality rate was recorded every 12 h in a 72 h interval. (b) The bacterial load of each group at 48 h. (c) On the 4th day after intradermal injection of the same dose of strains of the different MRSA groups, the mice were sacrificed to measure the area and volume of the infected abscess. (d) Heat map of virulence genes in MRSA ST9 and ST398 isolated in China and Germany.

additional *hysA*^{vSaβ} gene (DG29-WT and DG29-Δ*hysA*^{vSaβ}-*hysA*^{vSaβ}) was also significantly increased (Figure 7(c)). In the mouse skin infection model, we also observed that the mutants DG29-Δ*hysA*^{vSaβ}-pAM401 and DG29-Δ*hysA*^{chr}-Δ*hysA*^{vSaβ} had a significantly reduced ability of skin abscess formation compared with the wild-type strain DG29-WT ($p < 0.05$, Figure 7(d)). We further used other different CHN- and GER-MRSA ST9 and ST398 strains for additional testing of *Galleria mellonella* larva infection and mouse skin infection, and these results were similar to those obtained with the above-mentioned strains (Data not shown). Therefore, our results suggest that *hysA*^{vSaβ} plays a role in the pathogenicity of MRSA ST398.

Discussion

The clonal lineage MRSA ST9-SCC*mec*XII-t899 observed in China [11,19] was different from MRSA ST9 strains identified in other countries such as Germany (SCC*mec*IV-t1430), Thailand (SCC*mec*IX-t337), and Malaysia (SCC*mec*V-t4358) [20,21], and suggested that MRSA ST9-SCC*mec*XII-t899 had evolved independently in China and occupied the dominant position in Chinese pig population. In contrast, most CHN-MRSA ST398 strains belong to SCC*mec*Vc-t034, a most common LA-MRSA lineage in Europe, and have a close evolutionary relationship with European MRSA ST398, suggesting that CHN- and GER-MRSA ST398 might have evolved from the

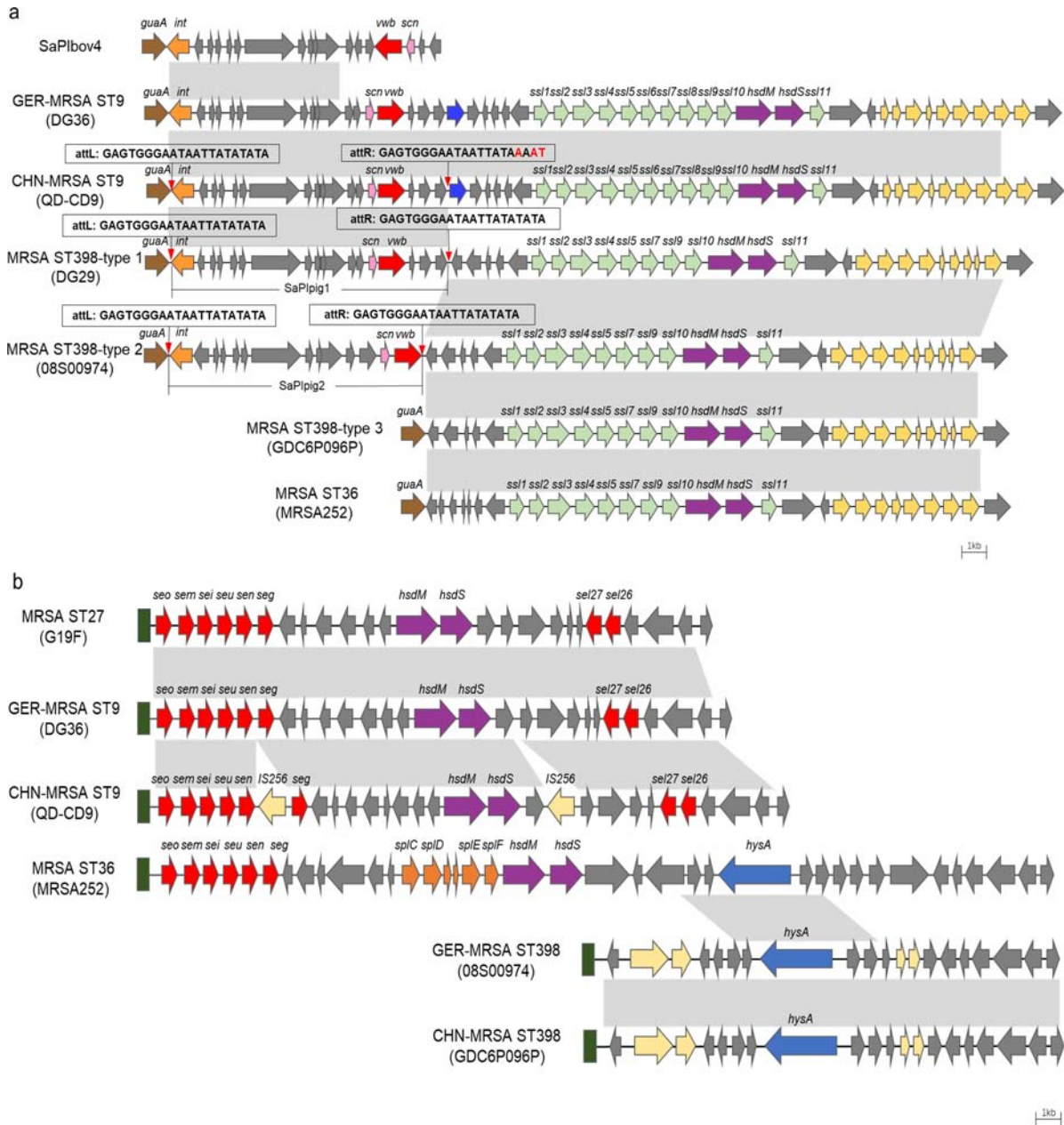


Figure 6. Analysis of the genomic structure of genomic islands vSa α and vSa β . (a) Comparative structural analyses of genomic island vSa α of the representative MRSA strains of ST9 and ST398 from both China and Germany against known sequence structure. (b) Comparative structural analyses of genomic island vSa β of the representative MRSA ST9 and ST398 strains from China and Germany with known structures. The coloured arrows represent genes that code for proteins with known function, and the grey arrows represent genes for putative proteins. Regions of 99% nucleotide sequence identity are indicated by grey shading. Red triangles indicate the location of DRs with the respective sequences shown in boxes. MRSA252 (GenBank number: BX571856), G19F (GenBank number: SZYN01000000).

same ancestor [22]. It should be noted that the MRSA ST398 has been proved to be transmitted through trade, human occupational exposure and livestock trucks, there are some successful cases of the introduction of MRSA ST398 from the positive regions to the negative regions [23,24]. Since 2008, according to data from China Customs, China has imported 4.76 million tons of pork from the EU, accounting for 61.8% of the total pork import volume, and the imported pork from Germany, Spain and Denmark accounted for 15.4%, 17.5% and 10.9%, respectively. We, therefore, speculate that the MRSA ST398 might

have been introduced into China from European countries, but the specific transmission route of MRSA ST398 in China needs further clarifications.

Compared with CHN- and GER-MRSA ST9, the genome of MRSA ST398 is more diverse, and genes with high dN/dS ratios are related to replication, repair, cell division, and defense mechanisms. These results suggest that MRSA ST398 undergoes more mutations or recombinations to adapt to different environmental conditions [25,26]. Besides, all MRSA ST398 lack the *hdsS* and *hdsM* genes of a type 1 restriction-modification (RM) system on the genomic island

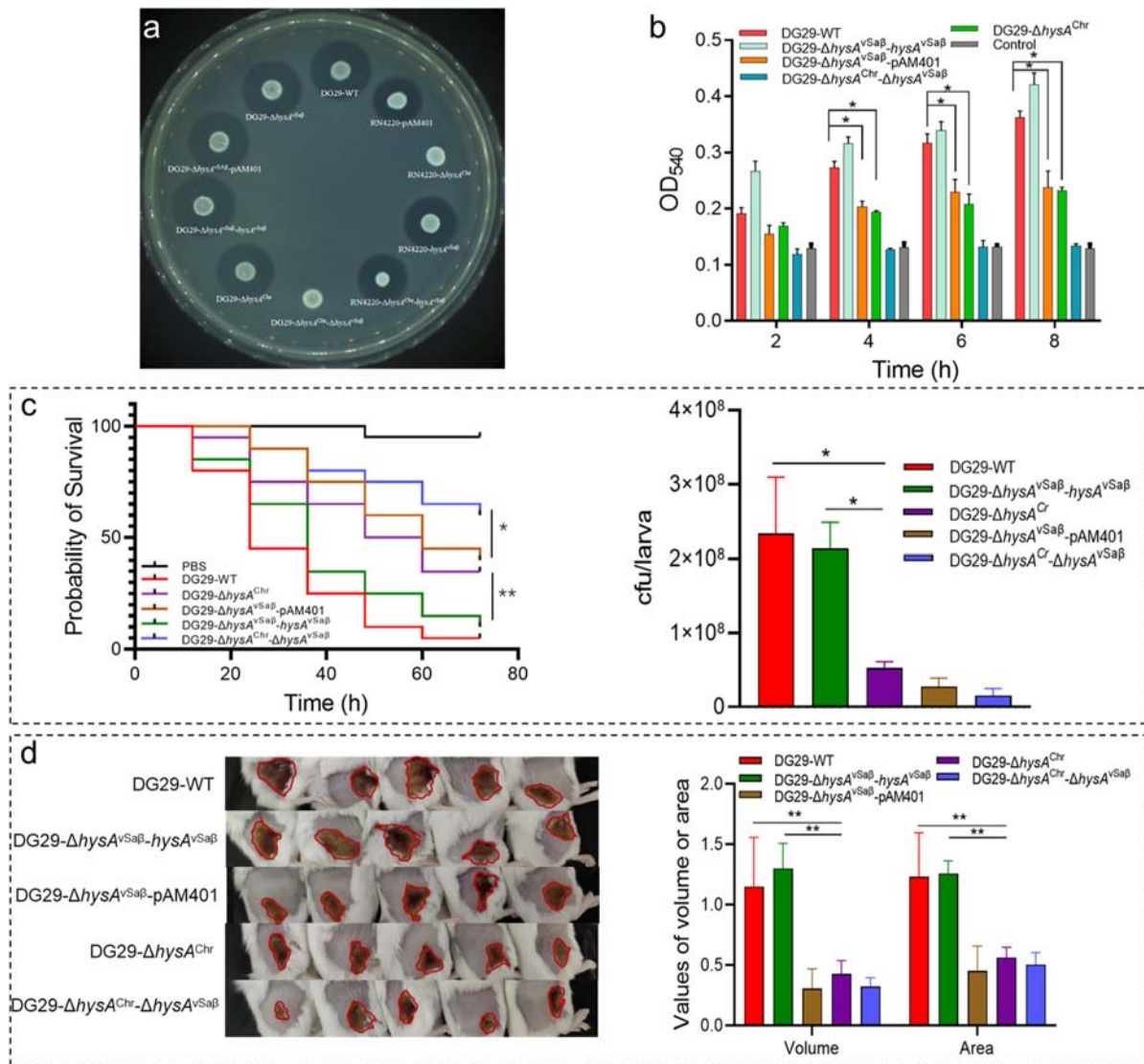


Figure 7. Functional verification of *hysA*^{vSaβ} gene. (a) The proteins encoded by *hysA* genes located in the chromosome and on genomic island vSaβ have the ability to hydrolyze HA. When both genes are knocked out, the ability to hydrolyze HA is lost. (b) Quantitative analysis showed that the *hysA*^{vSaβ} gene could significantly enhance the ability of HA hydrolysis. (c) Survival curve of *Galleria mellonella* larvae of *hysA*^{vSaβ} knockout or supplement strains and the bacterial load at 48 h. (d) On the 4th day after intradermal injection of the same dose of different groups of MRSA, the mice were sacrificed to measure the area and volume of the infected abscess.

vSaβ, which indicate that MRSA ST398 strains may easier acquire foreign genes [27]. In fact, we observed that two of the CHN-MRSA ST398 strains carried the *spw-lsa(E)-lnu(B)* resistance gene cluster, and the transposon-borne gene *fexA*, which indicated that the CHN-MRSA ST398 strains are adapting to the selection pressure imposed by the antimicrobial agents commonly used in the Chinese pig breeding industry. *In vitro* fitness tests showed that the CHN- and GER-MRSA ST398 strains were more resistant to acidic and hypertonic conditions than those belonging to ST9. This means that MRSA ST398 is more likely to survive and colonize acidic or hypertonic environments, such as the skin and the nasal cavity [28–31]. However, the specific molecular mechanism leading to the differences in fitness needs to be further explored. In addition, the growth advantages of CHN- and GER-

ST398 under co-cultivation conditions may be due to the fact that CHN-MRSA ST9 carried more AMR genes and thus, had a higher fitness cost [32]. Therefore, we may predict that MRSA ST398 will adapt to the complex Chinese pig breeding environment, as it can easier integrate foreign AMR genes, and has an improved fitness and competitiveness as compared to MRSA ST9.

Tetracycline, tiamulin, florfenicol as well as macrolides, lincosamides and streptogramins (MLS) are the most commonly used antimicrobial agents in pig industry in China, which may promote the successful selection of multidrug resistant CHN-MRSA ST9 strains [33,34]. A previous study has proved that GER-MRSA ST398 acquired *tet(K)* and *tet(M)* to better adapt to the selection pressure imposed by tetracycline commonly used in pig breeding [7]. We also

found that the dominant CHN-MRSA ST9 and the GER-MRSA ST398 revealed enhanced biofilm formation ability and desiccation resistance compared with their non-dominant counterparts. Biofilm production may protect the bacteria and allows them to survive in hostile or extreme environments, including desiccation [35,36]. All MRSA ST9 and most of the ST398 strains carried the *vwb*^{vSaa} gene on the genomic island vSaa. The Vwb^{vSaa} protein may not only play a part in ruminant specific host adaptability, but also involve in the colonization and transmission of MRSA ST398 and ST9 in pigs [15]. Previous studies also indicated the expression of *vwb*^{vSaa} is up-regulated in the process of pig nose tissue adhesion by MRSA ST398 [37]. In view of these characteristics, the selection pressure imposed by different antimicrobial agents plays a key role in the formation of dominant MRSA clones in China and Germany, the improved biofilm formation and desiccation resistance is supportive to the survival of dominant clones, and the novel SaPIpig1 and SaPIpig2 pathogenicity islands including the *vwb*^{vSaa} gene may contribute to the transmission of ST9 and ST398 between pigs in China and Germany, respectively.

Carrying a *hysA* homologous gene on the genomic island vSaβ seems to be a major feature of MRSA ST398, which has been reported in a previous study of MRSA ST398 isolated from cases of human endocarditis [38]. The *hysA* gene in the chromosomal DNA has been confirmed to play an important role in the virulence of *S. aureus* because it can indirectly inhibit the immune response by decomposing the host's hyaluronic acid, allowing bacteria to spread and proliferate [39]. To the best of our knowledge, we demonstrated, for the first time, the coexistence of *hysA*^{vSaβ} and the chromosome-borne *hysA*^{chr} gene, both mediating hyaluronidase activity. The *hysA*^{vSaβ} genes enhanced the host invasion ability of MRSA ST398 and possibly played an important role in the enhanced pathogenicity of MRSA ST398. However, the regulatory and immunological mechanisms of *HysA*^{vSaβ} in enhancing the virulence of MRSA ST398 need to be further studied.

In conclusion, we found that the selection pressure of florfenicol, tiamulin and MLS antimicrobial agents in China, and tetracyclines used in Germany may play a key role in the formation of the dominant clones CHN-MRSA ST9 and GER-MRSA ST398, respectively, and the presence of the coagulation gene *vwb*^{vSaa}, improved biofilm formation and resistance to desiccation also contribute to their survival and persistence in the pig host or harsh environment. Compared with MRSA ST9, MRSA ST398 can easier acquire foreign AMR genes, is more adaptable to acidic and hyperosmotic environments, and shows higher competitiveness, and thus, has the possibility to gradually become an epidemic clone in China. It

is worth noting that the unique *hysA*^{vSaβ} gene carried on the genomic island vSaβ enhances the pathogenicity of MRSA ST398, which may pose a greater threat to public health and should be closely monitored.

Materials and methods

Bacterial strains used in this study

A total of 81 non-duplicate *S. aureus* strains (ST9, *n* = 41 or ST398, *n* = 40) were used in the core genome SNP phylogenetic analysis (Table S11). The 51 (ST9, *n* = 26 or ST398, *n* = 25) MRSA/MSSA strains were obtained from pigs in various regions of Germany and China during the period between 2004 and 2016 [40,41], and the sequence data of the remaining 30 supplemental strains from other countries or sources were obtained from the NCBI public database. Briefly, 51 strains were randomly selected according to the principle of the most common genome characteristics and the most extensive coverage of collection sites. Five unrelated strains each of MRSA ST9 and ST398 isolated in China and Germany were randomly selected according to the results of core genome SNP phylogenetic analysis and antimicrobial resistance profiling for the whole genome comparison analysis and the *in vitro* phenotypic assays (Table S12). We further randomly selected one strain from each group for the *Galleria mellonella* larva virulence and mice skin infection assays (Table S12). The whole process of strain selection in this study is shown in supplemental Figure S1.

Whole genome sequencing and molecular analysis

300-bp paired-end reads with a minimum of 250-fold coverage for each strain were obtained following sequencing using the Illumina HiSeq X-Ten System. Sequence reads were assembled with SPAdes (version 3.12.0). GER-MRSA ST9 and CHN-MRSA ST398 representative strains DG36 (GenBank number: CP065199) and GDC6P096P (GenBank number: CP065194) were selected and sequenced by MinION device. High quality assembled sequences were obtained using Unicycler v0.4.8 by combining with short reads data after quality control processing. Assembled DNA sequences were run through an automatic annotation pipeline via RAST (<https://rast.nmpdr.org/>). Known alleles of AMR and virulence genes were screened using a direct read mapping approach implemented in SRST2 against the ResFinder and VirulenceFinder databases (>90% identity) [42]. Multi-locus sequence typing (MLST), SCCmec and *spa* typing of all strains were conducted by online analysis tools (<http://www.genomicepidemiology.org/>).

Phylogenetic analysis

Two phylogenetic trees based on core genome SNP analysis were constructed by Parsnp (version 1.2) using the default parameters in Harvest suite to assess the genetic relatedness of MRSA ST9 and ST398 from both China and Germany. CHN-MRSA ST9 strain QD-CD9 and GER-MRSA ST398 strain 08S00974 [43] served as the references, the bootstrap confidence values were generated using 1,000 permutations. The SNP information of each tree was analyzed by Harvest-Tools (version 1.2). The visual annotation of the phylogenetic trees was conducted using ITOL (<https://itol.embl.de/>).

Comparative genome analysis, COGs analyses based on SNPs and pan-genome analyses

The complete genome sequences of strains QD-CD9, 08S00974, GDC6P096P and DG36 were used as the reference sequences of the four groups of strains, and the BLAST Ring Image Generator (BRIG) was used for genome-wide comparison, the strains used are listed in Table S12. Single nucleotide polymorphisms (SNPs), substitutions and insertions/deletions (indels) were found using Snippy (version 3.0). To determine the functional gene categories of missense SNP-containing genes, we used eggNOG-mapper with HMM search mode to compare representative protein sequences with the eggNOG database (<http://eggnog5.embl.de/>). The database classifies proteins by their evolutionary relationship and allows further assignment of proteins into functional categories. Pan-genome analysis was carried out using Roary (version 3.11.2) to cluster the genes encoding complete protein sequences into core (hard core and soft core) and accessory (shell and cloud) genomes [44].

Antimicrobial susceptibility testing

Antimicrobial susceptibility testing was performed using the broth microdilution method according to the Clinical and Laboratory Standards Institute documents VET01S and M100-S30, and the 15 antimicrobial agents tested are given in the supplementary material.

Independent and competitive growth assay

Independent and competitive assays were carried out using the previously described methods [44]. The selective antibiotic used in the competition experiment and the calculation formula of the maximum growth rate (μ) are given in the supplementary material.

Biofilm formation assay

Briefly, according to the previous method, 20 μ L of bacterial log phase culture was added to 200 μ L tryptic soy broth (TSB) containing 0.25% glucose in 96-well flat-bottom microtiter plates and cultured at 37°C for 48 h, and then the biofilm formation of MRSA strains was detected by crystal violet staining [45]. The specific steps were given in the supplementary material.

Fitness assays of physical and chemical pressure

The physical and chemical pressures involved in this study include desiccation, acidic/alkaline pH, high osmolarity, hyperthermy and oxidation pressure. Briefly, the representative strains of MRSA ST9 and ST398 from China and Germany were cultured to mid-log phase and adjusted to an OD₆₀₀ of 0.2 (\pm 0.05), and then related assays were carried out according to the previous described method. The specific conditions and steps were given in the supplementary material.

Galleria mellonella larva virulence model and bacterial count tests

According to the previous method [46], strains were cultured to mid-log phase and adjusted to 1×10^7 cfu/mL. Groups of 13 *Galleria* larvae, additional three larvae were used for bacterial load investigation, were used for inoculation with 10 μ L PBS-washed strains, the control groups of 10 larvae were inoculated with 10 μ L sterile PBS. incubated at 37°C. All the larvae were incubated at 37°C, and the fatalities was recorded every 12 h for a 72 h interval. Living larva per infecting strain was homogenized and diluted properly, and *S. aureus* colonies were counted on a selective medium, supplemented with antimicrobial agents to which the respective infecting strain was resistant (Table S13).

Mouse model of *S. aureus* skin infection

Animal experiments were performed following the guidelines for the Care and Use of Laboratory Animals of the Chinese Association for Laboratory Animal Sciences. The animal protocol was approved by the ethics committee on animal experiments of China Agricultural University. According to the previous method, Balb/c female mice (6–8 weeks old, 20–25 g) were used for the skin infection model. Mice were anesthetized with 2% isoflurane and inoculated with 100 μ L PBS containing 1×10^7 live strains or PBS alone in the right flank by intradermal injection. After 4 days, the abscess length (L) and width (W) was measured with the calipers. The abscess length

and width dimensions were used to calculate the abscess volume [$V = 4/3\pi(L/2)^2 \times W/2$] and area [$A = \pi(L/2) \times W/2$] [47].

Coagulation assays

The coagulation assays were conducted as described previously [48]. Porcine, ovine and bovine plasmas with EDTA were used for the coagulation experiments. The tube coagulation assay was performed in 1.5 mL centrifuge tubes by mixing 300 μ L of diluted plasma with 1×10^8 of PBS-washed *S. aureus* bacteria. The tubes were incubated at 37°C, the level and time of coagulation was observed by tilting the tubes.

Protein modelling and functional verification of HysA^{vSa β} and HysA^{Chr}

Homology modelling of proteins HysA^{vSa β} and HysA^{Chr} were performed using the biomolecular simulation programme Amber14, using the crystal structure of the original *S. agalactiae* hyaluronidase (PDB accession number: 1F1S) as template. Molecular docking between crystal structure 1F1S, the modelled HysA^{vSa β} and HysA^{Chr} proteins, and hyaluronic acid (HA) were conducted using AutoDock 4.2.6. The binding energy of small molecules was calculated using the MM-PBSA module of Amber14 software.

To confirm the role of the gene *hysA*^{vSa β} , we used CRISPR RNA-guided cytidine deaminase (pnCasSA-BEC) base-editing system [49] and pAM401 expression plasmid to construct *hysA*^{chr} or/and *hysA*^{vSa β} knockout or/and complementary strains of MRSA ST398 strain DG29 and *S. aureus* RN4220, the specific constructed strains are shown in Table S14. Hyaluronidase activity of constructed strains was revealed by flooding the plate with 10% (w/v) cetylpyridinium chloride [39]. To quantitatively analyze the HA decomposing ability of each strain, hyaluronidase activity in culture supernatants was assayed by method of dinitrosalicylic acid reagent [39,50]. The aforementioned *Galleria mellonella* larva virulence model and mouse skin infection model were used to evaluate the role of *hysA*^{vSa β} in the MRSA ST398 clinical strain DG29.

Statistical analysis

Each experiment was repeated three times independently. Data were analyzed with the software SPSS version 20.0 and GraphPad Prism 7. Data concerning continuous variables such as resistance to physical-chemical stresses, competitive ability and virulence comparison were analyzed using a two-tailed non-parametric Student's *t*-test, or a one-way ANOVA test for more than two lineages. Comparisons of antimicrobial resistance rates and distribution of AMR

genes among strains were conducted using Fisher's exact test and Student's *t*-test. The survival data of *Galleria mellonella* larvae were analyzed with the Log-Rank test (Mantel-Cox). The value of $p < 0.05$ was considered to be statistically significant.

Disclosure statement

No potential conflict of interest was reported by the authors.

Funding

This work was supported by National Natural Science Foundation of China [grant numbers 31761133022, 81861138051]; German Research Foundation [grant number SCHW382/11-1].

References

- [1] Fitzgerald JR. Livestock-associated *Staphylococcus aureus*: origin, evolution and public health threat. Trends Microbiol. 2012;20(4):192–198.
- [2] Chuang Y, Huang Y. Livestock-associated methicillin-resistant *Staphylococcus aureus* in Asia: an emerging issue? Int J Antimicrob Agents. 2015;45(4):334–340.
- [3] Butaye P, Argudin MA, Smith TC. Livestock-associated MRSA and its current evolution. Curr Clin Microbiol Rep. 2016;3(1):19–31.
- [4] Parisi A, Caruso M, Normanno G, et al. MRSA in swine, farmers and abattoir workers in southern Italy. Food Microbiol. 2019;82:287–293.
- [5] Li W, Liu J, Zhang X, et al. Emergence of methicillin-resistant *Staphylococcus aureus* ST398 in pigs in China. Int J Antimicrob Agents. 2018;51(2):275–276.
- [6] Price LB, Stegger M, Hasman H, et al. *Staphylococcus aureus* CC398: host adaptation and emergence of methicillin resistance in livestock. Mbio. 2012;3(1):e305–e311.
- [7] Larsen J, Clasen J, Hansen JE, et al. Copresence of *tet(K)* and *tet(M)* in livestock-associated methicillin-resistant *Staphylococcus aureus* clonal complex 398 is associated with increased fitness during exposure to sublethal concentrations of tetracycline. Antimicrob Agents Chemother. 2016;60(7):4401–4403.
- [8] Larsen J, Petersen A, Larsen AR, et al. Emergence of livestock-associated methicillin-resistant *Staphylococcus aureus* bloodstream infections in Denmark. Clin Infect Dis. 2017;65(7):1072–1076.
- [9] Murra M, Mortensen KL, Wang M. Livestock-associated methicillin-resistant *Staphylococcus aureus* (clonal complex 398) causing bacteremia and epidural abscess. Int J Infect Dis. 2019;81:107–109.
- [10] Larsen J, Petersen A, Sorum M, et al. Methicillin-resistant *Staphylococcus aureus* CC398 is an increasing cause of disease in people with no livestock contact in Denmark, 1999 to 2011. Euro Surveill. 2015;20(37):10.2807.
- [11] Zhou W, Li X, Osmundson T, et al. WGS analysis of ST9-MRSA-XII isolates from live pigs in China provides insights into transmission among porcine, human and bovine hosts. J Antimicrob Chemother. 2018;73(10):2652–2661.
- [12] Yan X, Li Z, Chlebowicz MA, et al. Genetic features of livestock-associated *Staphylococcus aureus* ST9

- isolates from Chinese pigs that carry the *lsa(E)* gene for quinupristin/dalfopristin resistance. *Int J Med Microbiol.* 2016;306(8):722–729.
- [13] Wu Z, Li F, Liu D, et al. Novel type XII staphylococcal cassette chromosome *mec* harboring a new cassette chromosome recombinase, CcrC2. *Antimicrob Agents Chemother.* 2015;59(12):7597–7601.
- [14] Jin Y, Yu X, Chen Y, et al. Characterization of highly virulent community-associated methicillin-resistant *Staphylococcus aureus* ST9-SCC*mec* XII causing bloodstream infection in China. *Emerg Microbes Infect.* 2020;9(1):2526–2535.
- [15] Viana D, Blanco J, Tormo-Más MA, et al. Adaptation of *Staphylococcus aureus* to ruminant and equine hosts involves SaPI-carried variants of von Willebrand factor-binding protein. *Mol Microbiol.* 2010;77(6):1583–1594.
- [16] Sakwinska O, Giddey M, Moreillon M, et al. *Staphylococcus aureus* host range and human-bovine host shift. *Appl Environ Microb.* 2011;77(17):5908.
- [17] Ellington MJ, Hope R, Livermore DM, et al. Decline of EMRSA-16 amongst methicillin-resistant *Staphylococcus aureus* causing bacteraemias in the UK between 2001 and 2007. *J Antimicrob Chemother.* 2010;65(3):446–448.
- [18] Li S, Jedrzejewski MJ. Hyaluronan binding and degradation by *Streptococcus agalactiae* hyaluronate lyase. *J Biol Chem.* 2001;276(44):41407–41416.
- [19] Chen C, Lauderdale TY, Lu C, et al. Clinical and molecular features of MDR livestock-associated MRSA ST9 with staphylococcal cassette chromosome *mecXII* in humans. *J Antimicrob Chemother.* 2018;73(1):33–40.
- [20] Neela V, Mohd Zafrul A, Mariana NS, et al. Prevalence of ST9 methicillin-resistant *Staphylococcus aureus* among pigs and pig handlers in Malaysia. *J Clin Microbiol.* 2009;47(12):4138–4140.
- [21] Larsen J, Imanishi M, Hinjoy S, et al. Methicillin-resistant *Staphylococcus aureus* ST9 in pigs in Thailand. *Plos One.* 2012;7(2):e31245.
- [22] Witte W, Strommenger B, Stanek C, et al. Methicillin-resistant *Staphylococcus aureus* ST398 in humans and animals, Central Europe. *Emerg Infect Dis.* 2007;13(2):255–258.
- [23] Grøntvedt CA, Elstrøm P, Stegger M, et al. Methicillin-Resistant *Staphylococcus aureus* CC398 in humans and pigs in Norway: a “One health” perspective on introduction and transmission. *Clin Infect Dis.* 2016;63(11):1431–1438.
- [24] Pirolo M, Sieber RN, Moodley A, et al. Local and transboundary transmissions of methicillin-resistant *Staphylococcus aureus* sequence type 398 through pig trading. *Appl Environ Microb.* 2020;86(13):e00430–20.
- [25] Lindsay JA. *Staphylococcus aureus* genomics and the impact of horizontal gene transfer. *Int J Med Microbiol: IJMM.* 2014;304(2):103–109.
- [26] Uhlemann A, Mcadam PR, Sullivan SB, et al. Evolutionary dynamics of pandemic methicillin-sensitive *Staphylococcus aureus* ST398 and its international spread via routes of human migration. *Mbio.* 2017;8(1):e1316–e1375.
- [27] Waldron DE, Lindsay JA. *SauI*: a novel lineage-specific type I restriction-modification system that blocks horizontal gene transfer into *Staphylococcus aureus* and between *S. aureus* isolates of different lineages. *J Bacteriol.* 2006;188(15):5578–5585.
- [28] Proksch E. Ph in nature, humans and skin. *J Dermatol.* 2018;45(9):1044–1052.
- [29] England RJ, Homer JJ, Knight LC, et al. Nasal pH measurement: a reliable and repeatable parameter. *Clin Otolaryngol Allied Sci.* 1999;24(1):67–68.
- [30] Summerfield A, Meurens F, Ricklin ME. The immunology of the porcine skin and its value as a model for human skin. *Mol Immunol.* 2015;66(1):14–21.
- [31] Jantsch J, Schatz V, Friedrich D, et al. Cutaneous Na⁺ storage strengthens the antimicrobial barrier function of the skin and boosts macrophage-driven host defense. *Cell Metab.* 2015;21(3):493–501.
- [32] Vogwill T, Maclean RC. The genetic basis of the fitness costs of antimicrobial resistance: a meta-analysis approach. *Evol Appl.* 2015;8(3):284–295.
- [33] Krishnasamy V, Otte J, Silbergeld E. Antimicrobial use in Chinese swine and broiler poultry production. *Antimicrob Resist Infect Control.* 2015;4:17.
- [34] Zhang Q, Ying G, Pan C, et al. Comprehensive evaluation of antibiotics emission and fate in the river basins of China: source analysis, multimedia modeling, and linkage to bacterial resistance. *Environ Sci Technol.* 2015;49(11):6772–6782.
- [35] Tahir S, Chowdhury D, Legge M, et al. Transmission of *Staphylococcus aureus* from dry surface biofilm (DSB) via different types of gloves. *Infect Control Hosp Epidemiol.* 2019;40(1):60–64.
- [36] Moormeier DE, Bayles KW. *Staphylococcus aureus* biofilm: a complex developmental organism. *Mol Microbiol.* 2017;104(3):365–376.
- [37] Tulinski P, Duim B, Wittink FR, et al. *Staphylococcus aureus* ST398 gene expression profiling during ex vivo colonization of porcine nasal epithelium. *BMC Genomics.* 2014;15(215):915.
- [38] Schijffelen MJ, Boel CHE, van Strijp JAG, et al. Whole genome analysis of a livestock-associated methicillin-resistant *Staphylococcus aureus* ST398 isolate from a case of human endocarditis. *BMC Genomics.* 2010;11:376.
- [39] Makris G, Wright JD, Ingham E, et al. The hyaluronate lyase of *Staphylococcus aureus* - a virulence factor? *Microbiology (Reading).* 2004;150(Pt 6):2005–2013.
- [40] Kadlec K, Ehrlich R, Monecke S, et al. Diversity of antimicrobial resistance pheno- and genotypes of methicillin-resistant *Staphylococcus aureus* ST398 from diseased swine. *J Antimicrob Chemother.* 2009;64(6):1156–1164.
- [41] Li J, Jiang N, Ke Y, et al. Characterization of pig-associated methicillin-resistant *Staphylococcus aureus*. *Vet Microbiol.* 2017;201:183–187.
- [42] Inouye M, Dashnow H, Raven L, et al. SRST2: rapid genomic surveillance for public health and hospital microbiology labs. *Genome Med.* 2014;6(11):90.
- [43] Makarova O, Johnston P, Walther B, et al. Complete genome sequence of the livestock-associated methicillin-resistant strain *Staphylococcus aureus* subsp. *aureus* 08S00974 (Sequence Type 398). *Genome Announc.* 2017;5(19):e00294–17.
- [44] Page AJ, Cummins CA, Hunt M, et al. Roary: rapid large-scale prokaryote pan genome analysis. *Bioinformatics.* 2015;31(22):3691–3693.
- [45] Haney EF, Trimble MJ, Hancock REW. Microtiter plate assays to assess antibiofilm activity against bacteria. *Nat Protoc.* 2021;16(5):2615–2632.
- [46] Richards RL, Haigh RD, Pascoe B, et al. Persistent *Staphylococcus aureus* isolates from two independent

- cases of bacteremia display increased bacterial fitness and novel immune evasion phenotypes. *Infect Immun.* **2015**;83(8):3311–3324.
- [47] Malachowa N, Kobayashi SD, Braughton KR, et al. Mouse model of *Staphylococcus aureus* skin infection. *Methods Mol Biol.* **2013**;1031:109–116.
- [48] Viana D, Blanco J, Tormo-Más MA, et al. Adaptation of *Staphylococcus aureus* to ruminant and equine hosts involves SaPI-carried variants of von Willebrand factor-binding protein. *Mol Microbiol.* **2010**;77(6):1583–1594.
- [49] Gu T, Zhao S, Pi Y, et al. Highly efficient base editing in *Staphylococcus aureus* using an engineered CRISPR RNA-guided cytidine deaminase. *Chem Sci.* **2018**;9(12):3248–3253.
- [50] Miller GL. Use of dinitrosalicylic acid reagent for determination of reducing sugar. *Anal Chem.* **1959**;31(3):426–428.